NEUTRON STAR MERGER

Early spectra of the gravitational wave source GW170817: Evolution of a neutron star merger

B. J. Shappee,[1,2]* J. D. Simon,[1] M. R. Drout,[1] A. L. Piro,[1] N. Morrell,[3] J. L. Prieto,[4,5] D. Kasen,[6,7] T. W.-S. Holoien,[1] J. A. Kollmeier,[1] D. D. Kelson,[1] D. A. Coulter,[8] R. J. Foley,[8] C. D. Kilpatrick,[8] M. R. Siebert,[8] B. F. Madore,[1] A. Murguia-Berthier,[8] Y.-C. Pan,[8] J. X. Prochaska,[8] E. Ramirez-Ruiz,[8,9] A. Rest,[10,11] C. Adams,[12] K. Alatalo,[1,10] E. Bañados,[1] J. Baughman,[4,13] R. A. Bernstein,[1] T. Bitsakis,[14] K. Boutsia,[3] J. R. Bravo,[3] F. Di Mille,[3] C. R. Higgs,[15,16] A. P. Ji,[1,11] G. Maravelias,[17] J. L. Marshall,[18] V. M. Placco,[19] G. Prieto,[3] Z. Wan[20]

On 17 August 2017, Swope Supernova Survey 2017a (SSS17a) was discovered as the optical counterpart of the binary neutron star gravitational wave event GW170817. We report time-series spectroscopy of SSS17a from 11.75 hours until 8.5 days after the merger. Over the first hour of observations, the ejecta rapidly expanded and cooled. Applying blackbody fits to the spectra, we measured the photosphere cooling from $11{,}000^{+3400}_{-900}$ to 9300^{+300}_{-300} kelvin, and determined a photospheric velocity of roughly 30% of the speed of light. The spectra of SSS17a began displaying broad features after 1.46 days and evolved qualitatively over each subsequent day, with distinct blue (early-time) and red (late-time) components. The late-time component is consistent with theoretical models of r-process–enriched neutron star ejecta, whereas the blue component requires high-velocity, lanthanide-free material.

Short gamma-ray bursts (GRBs) have long been hypothesized to be produced by neutron star mergers (*1*, *2*), and thus they are the most likely electromagnetic counterparts to the gravitational wave signals from binary neutron star coalescence. Unfortunately, because GRB emission is highly nonisotropic (*3*), in many cases the beam of gamma rays will not be seen by an observer. This has motivated studies of electromagnetic counterparts that are more isotropic, with one of the most popular cases being the so-called macronovae or kilonovae (*4*–*8*). These transients would result from the outflow of ~0.01 solar masses of neutron-rich material, ejected from the merging neutron stars at $\gtrsim$10% of the speed of light. This neutron-rich material is expected to synthesize heavy elements that power a fast transient peaking at red optical or near-infrared (near-IR) wavelengths via their radioactive decay. Furthermore, the r-process nucleosynthesis in these outflows—named from the capture of neutrons onto lighter seed nuclei on a timescale more rapid than β decays (*9*, *10*)—may explain the origin of half of the elements heavier than iron in the periodic table (*11*, *12*). Although a handful of candidate kilonovae following short GRBs have been identified (*13*–*15*), none have been studied in detail or conclusively confirmed.

The overall heating rate from r-process nucleosynthesis is generally agreed upon and fairly robust with respect to the composition (*6*, *7*), but the expected spectroscopic appearance of a kilonova is much less clear. Kilonova spectra depend strongly on the nuclear yields, neutrino flux, geometric orientations, mass, and velocity of the ejecta. The neutron-rich outflow is expected to produce elements in the lanthanide series, which have a large effect on the emergent radiation because of the opacity generated by their numerous bound-bound electronic transitions (*16*). Despite considerable theoretical effort, there is no consensus on the expected spectrum of a kilonova (*16*–*18*). There could be multiple components to the ejecta, with different compositions, opacities, geometries, and velocities (*19*). In the absence of observational measurements of kilonovae, especially spectroscopy, this variety of theoretical models remains largely unconstrained.

On 17 August 2017, the Laser Interferometer Gravitational-Wave Observatory (LIGO) and Virgo Collaboration (LVC) detected GW170817, a gravitational wave (GW) signal from a binary neutron star merger (*20*). A contemporaneous and weak short GRB was detected by the *Fermi* spacecraft and International Gamma-Ray Astrophysics Laboratory (INTEGRAL) telescopes (*21*, *22*). Following the GW trigger, our One-Meter Two-Hemispheres (1M2H) collaboration identified an optical counterpart, Swope Supernova Survey 2017a (SSS17a), 10.87 hours after the merger (*23*, *24*). SSS17a was located in the galaxy NGC 4993 (*23*, *24*), at a distance of 40 Mpc (*25*), which is an order of magnitude closer than previous gravitational wave detections. This discovery was immediately announced to the LVC, and we began a comprehensive follow-up campaign that extended for nearly 3 weeks. A companion paper presents extensive ultraviolet (UV), optical, and near-IR photometry of SSS17a, following the light curve of SSS17a as it reddened and faded (*26*).

At 11.75 hours after the GW170817 trigger, we obtained an optical spectrum of SSS17a with the Low Dispersion Survey Spectrograph 3 (LDSS-3) on the Magellan-Clay telescope at the Las Campanas Observatory in Chile. This early spectrum shows a smooth blue continuum extending over the entire optical-wavelength range (Fig. 1) (*27*). In the next hour, we obtained three additional spectra at higher resolution using LDSS-3 and the Magellan Echellette (MagE) spectrograph on the Magellan-Baade telescope before SSS17a set and was no longer observable from Chile. The transient faded measurably at the bluest wavelengths during the short time interval covered by these initial spectra, whereas the spectra redward of 5000 Å did not evolve in this time span (Fig. 1).

Motivated by the fact that the UV-optical spectral energy distribution observed 3 to 4 hours later (at t = 0.67 days after the merger) is well approximated by a blackbody (*26*), we fit blackbody models to the observed rest-frame, dereddened spectra to quantify the very early spectral evolution (*28*). The best-fitting model results in a temperature of $11{,}000^{+3400}_{-900}$ K and radius of $3.3^{+0.3}_{-0.8} \times 10^{14}$ cm at t = 0.49 days. The

---

[1] The Observatories of the Carnegie Institution for Science, 813 Santa Barbara Street, Pasadena, CA 91101, USA. [2] Institute for Astronomy, University of Hawai'i, 2680 Woodlawn Drive, Honolulu, HI 96822, USA. [3] Las Campanas Observatory, Carnegie Observatories, Casilla 601, La Serena, Chile. [4] Núcleo de Astronomía de la Facultad de Ingeniería y Ciencias, Universidad Diego Portales, Avenida Ejército 441, Santiago, Chile. [5] Millennium Institute of Astrophysics, Santiago, Chile. [6] Departments of Physics and Astronomy, 366 LeConte Hall, University of California–Berkeley, Berkeley, CA 94720, USA. [7] Nuclear Science Division, Lawrence Berkeley National Laboratory, Berkeley, CA 94720, USA. [8] Department of Astronomy and Astrophysics, University of California–Santa Cruz, Santa Cruz, CA 95064, USA. [9] Dark Cosmology Center, Niels Bohr Institute, University of Copenhagen, Blegdamsvej 17, 2100 Copenhagen, Denmark. [10] Space Telescope Science Institute, 3700 San Martin Drive, Baltimore, MD 21218, USA. [11] Department of Physics and Astronomy, The Johns Hopkins University, 3400 North Charles Street, Baltimore, MD 21218, USA. [12] Division of Physics, Mathematics, and Astronomy, California Institute of Technology, Pasadena, CA 91125, USA. [13] Massachusetts Institute of Technology, Cambridge, MA 02139, USA. [14] Instituto de Radioastronomía y Astrofísica, Universidad Nacional Autónoma de México, C.P. 58190, Morelia, Mexico. [15] University of Victoria, Victoria, BC V8P 5C2, Canada. [16] National Research Council (NRC) Herzberg Institute of Astrophysics, 5071 West Saanich Road, Victoria, BC V9E 2E7, Canada. [17] Instituto de Física y Astronomía, Universidad de Valparaíso, Valparaíso, Chile. [18] George P. and Cynthia Woods Mitchell Institute for Fundamental Physics and Astronomy and Department of Physics and Astronomy, Texas A&M University, College Station, TX 77843, USA. [19] Department of Physics and Joint Institute for Nuclear Astrophysics (JINA) Center for the Evolution of the Elements, University of Notre Dame, Notre Dame, IN 46556, USA. [20] Sydney Institute for Astronomy, School of Physics, A28, University of Sydney, NSW 2006, Australia.
***Corresponding author. Email: shappee@hawaii.edu**

Fig. 1. Early optical spectra of SSS17a. Magellan-LDSS-3 and Magellan-MagE spectra of SSS17a acquired 11.75 and 12.75 hours after the LVC trigger, respectively. The overall slope of the continuum evolved subtly, but substantially, in this 1-hour interval, demonstrating a change in the effective temperature of the source. Blackbody models and uncertainties are shown by the shaded green (LDSS-3) and brown (MagE) regions. The thick and thin solid lines in the fit regions indicate the median and 90% confidence interval for the fits, respectively. These fits are described in (*28*). The shaded gray outlines surrounding each spectrum indicate the uncertainties on the flux-calibrated spectra. Although the MagE spectrum extends to 10,100 Å, we only use the data blueward of 7000 Å for the blackbody fit because of the difficulty of flux-calibrating the data at redder wavelengths where the overlap between adjacent spectral orders is minimal and telluric absorption bands can cover a large fraction of an order. A vertical offset of −0.35 dex has been applied to the MagE spectrum for clarity.

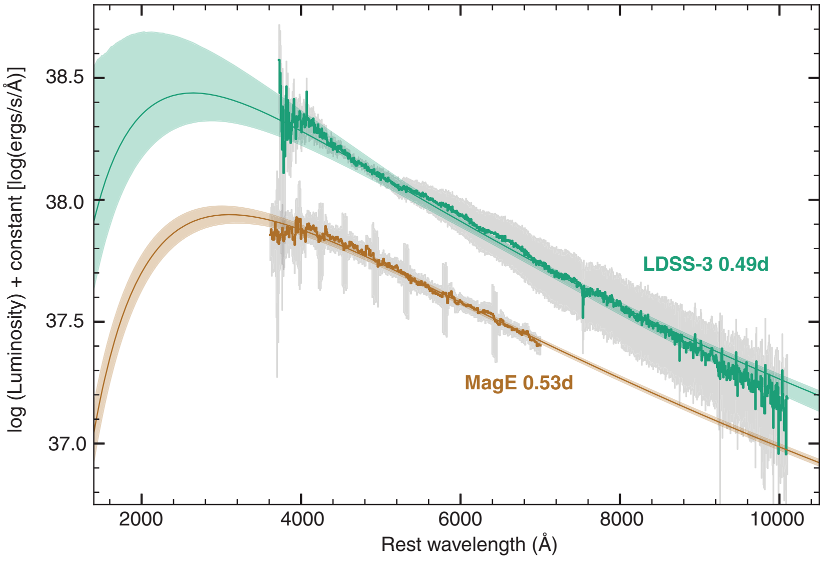

listed uncertainties represent 90% confidence intervals. Although the peak of the blackbody is located at UV wavelengths that we do not observe, the combination of the known luminosity and the spectral slope from 3800 to 10,000 Å provides sufficient constraints on the temperature. For material to reach this radius so quickly requires an expansion velocity of $77{,}000^{+7000}_{-20{,}000}$ km s^{-1}, or $0.26^{+0.02}_{-0.07}c$, where c is the speed of light. By comparison, typical supernovae have bulk velocities of 10,000 km s^{-1}. Even the most energetic supernovae, which are associated with long-duration GRBs, have peak measured photospheric velocities of ~20,000 to 50,000 km s^{-1} at 2 to 3 days postexplosion (*29*), less than what we infer here for the GW counterpart. Although the velocity of these systems may be even higher in the first day postexplosion, early spectra within 24 hours of explosion are not widely available for GRB supernovae.

For the MagE spectrum at $t = 0.53$ days, we fit a blackbody temperature of 9300^{+300}_{-300} K and radius of $4.1^{+0.2}_{-0.2} \times 10^{14}$ cm. The uncertainties on the temperature fits are not normally distributed, but we find that the difference in temperature between the LDSS-3 and MagE spectra is significant at 5σ confidence. This drop in temperature over only 1 hour indicates that the expanding ejecta are cooling rapidly. A similar velocity of $90{,}000^{+4000}_{-4000}$ km s^{-1} ($0.30^{+0.01}_{-0.01}c$) is inferred from this spectrum.

On subsequent nights, we acquired optical spectroscopy of SSS17a covering more than 1 week postexplosion using both Magellan telescopes. Most of the spectra were obtained with LDSS-3, but we also observed the source with the Inamori Magellan Areal Camera and Spectrograph (IMACS) and the Magellan Inamori Kyocera Echelle (MIKE) spectrograph. Our spectroscopic time series of SSS17a spans from 0.49 to 8.46 days after the GW170817 trigger (Fig. 2). A description of the acquisition and reduction of these spectra and a log of all spectroscopic observations are presented in the supplementary materials (*28*).

We searched the higher-resolution MIKE and MagE spectra for absorption or emission lines from the host galaxy, as well as for Na I D absorption from the Milky Way. Using the strength of the Milky Way Na I D absorption, we confirmed the foreground reddening that was determined using other spatially coarser methods (*28*). Host-galaxy features have been detected in all available short GRB spectra (*30*–*33*). However, we did not detect any host-galaxy lines;

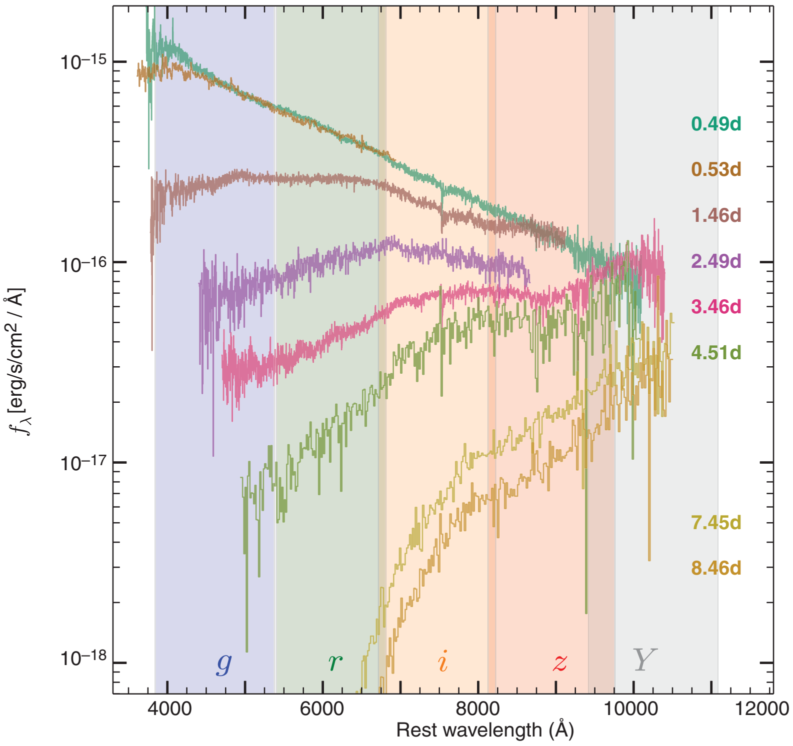

Fig. 2. Spectroscopic time series of SSS17a. The vertical axis is observed flux (f_λ). Observations began ~0.5 days after the merger and were obtained with the LDSS-3, MagE spectrograph, and the Inamori Magellan Areal Camera and Spectrograph (IMACS) on the Magellan telescopes. These spectra have been calibrated to the photometry of (*24*, *26*). Colored bands indicate the wavelength ranges of the *g*, *r*, *i*, *z*, and *Y* photometric filters.

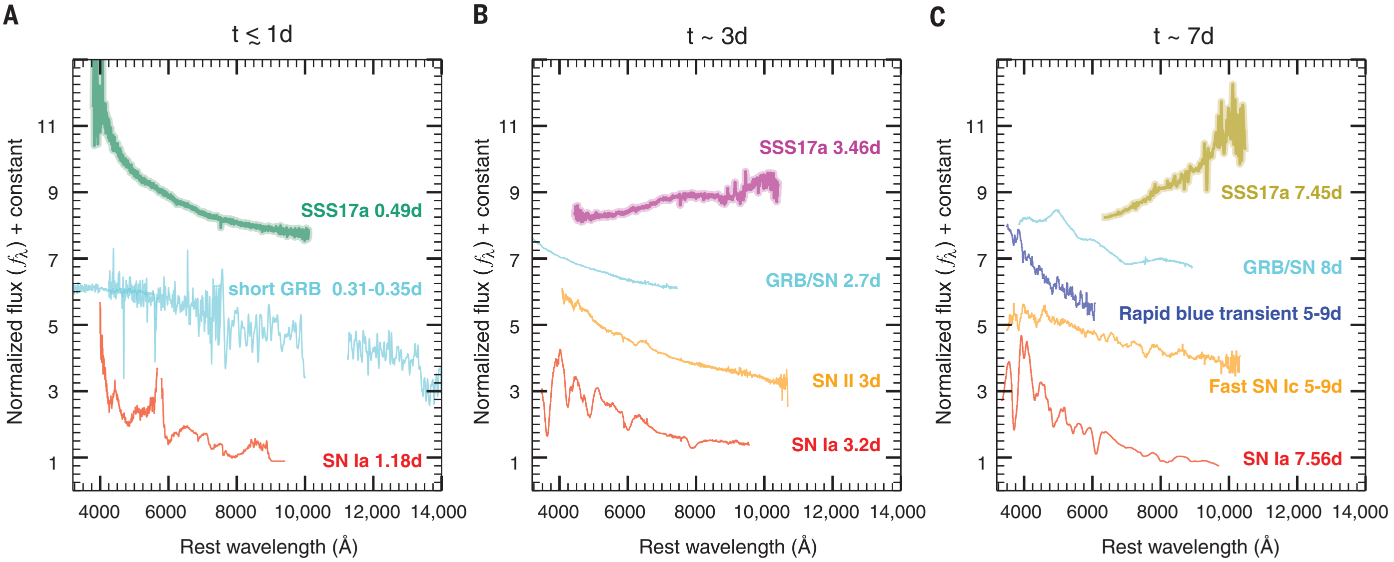

Fig. 3. Spectra of SSS17a compared with a broad range of other astronomical transients at several evolutionary phases. Although the ~0.5-day spectrum of SSS17a has few features and is potentially an extreme version of some other hot and/or fast transients, it evolves rapidly in comparison. Within 3 days of the LIGO trigger, the optical spectrum of SSS17a is no longer similar to other known transients. Phases listed are relative to the time of explosion for all objects. All spectra are divided by their median value and displayed with arbitrary additive offsets for clarity. (**A**) SSS17a compared to the type Ia supernova (SN Ia) SN2011fe (*42*) and the afterglow spectrum of the short gamma-ray burst GRB130603B (*33*). Few observations of other transients within 1 day of explosion are available. (**B**) SSS17a at 3.46 days after explosion compared to the SN Ia ASASSN-14lp (*43*), the type II supernova SN2006bp (*44*), and the long GRB and its associated afterglow and broad-lined type Ic supernova GRB030329/SN2003dh (*38*) at similar times relative to explosion. (**C**) SSS17a at 7.45 days after explosion compared to SN2011fe (*45*), the rapid blue transient PS1-12bv (*36*), the fast type Ic supernova SN2005ek (*46*), and the GRB/SN GRB980425/SN1998bw (*37*).

our 2σ limits on Na I D absorption are more than five times stricter than the absorption detected in GRB130603B (*28*, *33*).

After being observed as a rapidly cooling blackbody observed on the first night, later spectra show that the appearance of SSS17a changed not just quantitatively but also qualitatively each night. At 1.46 days, a broad feature extends from ~5000 to 7000 Å, and the spectrum declines toward shorter wavelengths. At 2.49 days, the peak wavelength of the emission has shifted to ~7500 Å, and the spectrum has a distinct triangular shape. At 3.46 and 4.51 days, the fall-off at blue wavelengths steepens, the peak of the optical emission continues evolving redward, and a new feature that increases with wavelength develops in the near-IR part of the spectrum. By 7.45 days after the merger, the spectrum consists of a smooth red continuum, with very little flux detected below 6500 Å. These data reveal that the photosphere continued expanding and cooling, with its temperature declining by a factor of ~4 within a week (*26*).

The spectral features of SSS17a become more complex over time. After the first night, they are not well described by either single-blackbody fits or the sum of two blackbodies. All features in the data are smooth and very broad, ~2500 Å wide for the peak centered at ~7500 Å in the 2.49- and 3.46-day spectra, ~2000 Å wide for the trough centered at ~9000 Å in the 2.49- and 3.46-day spectra, and >1000 Å for the near-IR feature at 3.46 and 4.51 days. It is not clear from the data whether these features should be interpreted as emission centered at the wavelength of the flux maxima or absorption centered on the flux minima. In either case, from their width and the Doppler effect, we can estimate that the material in SSS17a must be moving at a velocity of ~0.2c to 0.3c, which is consistent with the observed lack of narrow lines.

The photometric evolution of SSS17a strongly suggests two distinct components to the ejecta (*26*, *34*). The spectral evolution, as well as the inability to match the early- and late-time spectra with a single kilonova model, for which we make direct comparisons below, also favors two components. The largely featureless blue component dominates the initial spectrum but quickly fades within the first few days. After 3 days, the spectrum becomes dominated by a red component, corresponding to cooler temperatures, which fades much more slowly.

The spectral evolution of SSS17a is unlike known astronomical transients, as can be seen in Fig. 3, which compares the Magellan spectra taken at t = 0.49, 3.46, and 7.45 days after the GW170817 trigger to other classes of transients. Because SSS17a was associated with a short gamma-ray transient (*21*, *22*), it is natural to investigate whether the SSS17a spectra are consistent with afterglow emission. Only three short GRBs (all at redshifts $z > 0.3$) have available optical spectroscopy (*30*–*33*), of which only GRB130603B (*32*, *33*) is unambiguously classified as a short GRB. In Fig. 3, we show spectra of GRB130603B taken ~8 hours after the GRB (*33*), which do not resemble those of SSS17a. Unfortunately, there are no spectra of short GRBs reported in the literature at epochs later than 1 day. We therefore cannot compare our later spectra against other short GRBs at similar epochs. Despite the limited comparison sample, we conclude that the early blue spectrum of SSS17a does not resemble previously detected short GRB spectra, which are likely dominated by afterglows from a jet projected along the line of sight. Instead, we argue that the observations probe emission that is independent of the GRB. This conclusion is bolstered by the lack of x-ray and radio emissions at early times, which rules out a broadband synchrotron spectrum as the primary driver of the optical emission (*35*).

In Fig. 3, we also compare SSS17a to supernovae and other rapid transients. Type Ia and type Ibc supernovae develop emission lines with characteristic widths and velocities of 10,000 km s^{-1} (0.03c) and evolve over weeks to months rather than days. Young type II supernovae can have blue, smooth spectra, not dissimilar to the earliest spectra of SSS17a, but this phase lasts for many days. Later in their evolution, they settle to a temperature of ~6000 K for ~100 days, as determined by hydrogen recombination, and show hydrogen absorption lines, both of which are properties very much unlike those of SSS17a. Early spectra of rapid blue transients (*36*) can be as blue as SSS17a, but

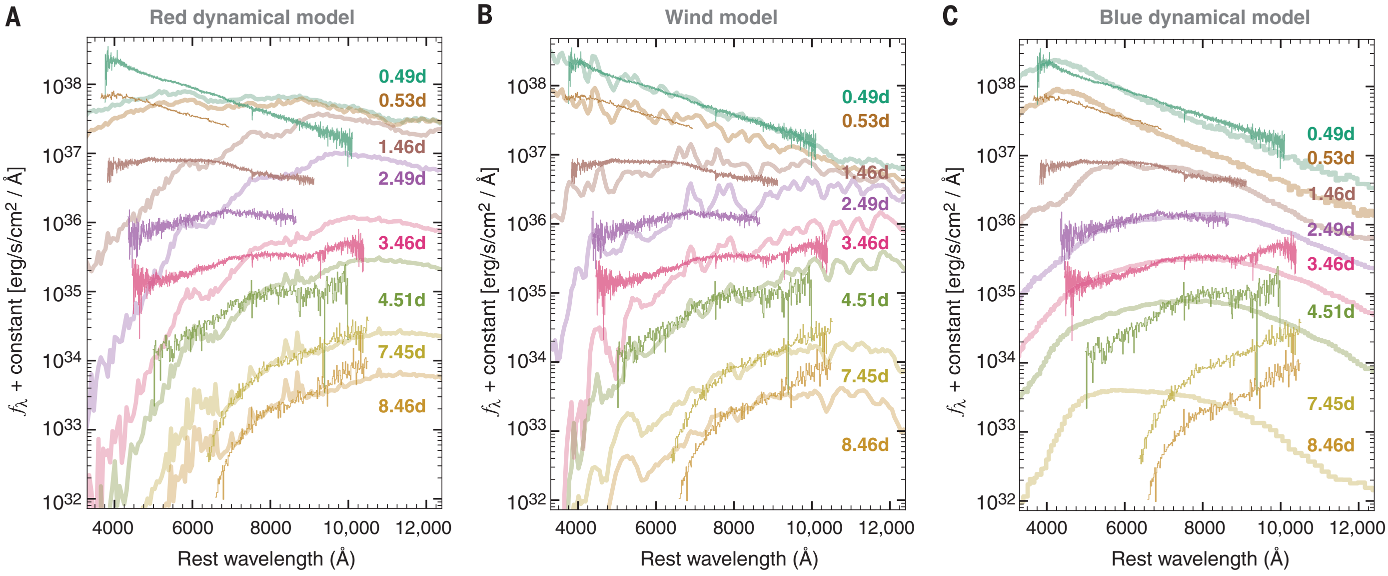

Fig. 4. Comparison of SSS17a to theoretical models. The vertical axis is observed flux (f_λ). The models shown are for three possible physical interpretations of SSS17a. Although the red kilonova model provides a reasonable likeness to the data at late times, the early-time spectra and kinematics require lanthanide-free relativistic material. No single model shown here or described in the current literature can self-consistently reproduce the full spectroscopic time series of SSS17a. (**A**) Lanthanide-rich red kilonova model from a neutron star merger and dynamical ejection (*17*). At each epoch, the absolute luminosity is scaled to match the data. (**B**) Disk-wind model (*19*) with a neutron star that immediately collapses after the merger. The absolute luminosity is scaled by a factor of ≳10 at each epoch to match the data. (**C**) Lanthanide-poor blue kilonova model from a neutron star merger and dynamical ejection (*41*). The model has been crafted to match the observations at early times (*34*).

they maintain their blue color for days, whereas SSS17a had become much redder by day 2.49. GRB980425/SN1998bw and GRB030329/SN2003dh, supernovae associated with long GRBs, revealed the spectrum of a type Ic supernova as the afterglow faded and remained detectable for months (*37*, *38*). However, the supernova features seen in GRB980425 are absent in SSS17a, and SSS17a again evolves and fades much faster, becoming undetectable in weeks.

Detailed comparison of the spectral features of SSS17a to theoretical models is challenging. Current models use only a small subset of the elements synthesized in the neutron-rich outflows, and, even for the elements that are included, there is considerable uncertainty in the details of their line transitions (*16*, *18*). The features that are found in the optical spectra of current models are composed of many different transitions and cannot be reliably associated with specific elements. We therefore focus on the most robust physical features (such as color, velocity, and temporal evolution) in our comparison.

The ejecta from a neutron star merger can have different compositions and velocities depending on their origin. This motivates comparisons to a few characteristic models. In Fig. 4A, we present theoretical models of 0.1 solar masses of lanthanide-rich material that has been dynamically ejected with a velocity of 0.2*c* (*17*). Such a model is consistent with the power-law evolution of the bolometric luminosity of SSS17a at times ≳4 days, which is consistent with the expectations for r-process heating (*26*), although it is not currently possible to identify the particular r-process elements responsible. Modest scaling, by a factor ≲7, was required to match the overall luminosity of each epoch, but there are qualitative similarities to the spectra from 4.51 days onward. However, this model alone does not reproduce the rapidly evolving early blue phase.

The material generating the early component is likely lanthanide-free to reproduce the blue emission. Such material can be driven by accretion disk winds (*39*) or dynamical ejection from the neutron star–neutron star merger interface (*40*). We consider both cases, with the main difference being the velocity of the material. In Fig. 4B, we compare SSS17a with a disk-wind model (*19*), which, although the model can account for the blue colors at early times, has a number of problems. These include a luminosity that is much too low (the model spectra have been scaled by over one order of magnitude), velocities (≲0.1*c*) that are much smaller than those we infer from the temperature evolution, and absorption features that are not seen in our early smooth spectra. We therefore disfavor a disk-wind origin.

For the case of lanthanide-free dynamical ejecta, there are fewer theoretical predictions of spectra available for direct comparison. We replicate the main features of this scenario with a model composed of fast-moving (≳0.2*c*) lanthanide-free material (*41*), shown in Fig. 4C. Unlike the previous scenarios, such a model may explain the spectra blueward of 9000 Å for times up to 3.46 days. At later epochs, the observed spectra have large red excesses relative to the model, which could be explained if the red component is obscuring the lanthanide-free material as the ejecta evolve (*34*). Such obscuration could occur because the red dynamical ejecta are more concentrated in equatorial regions, whereas the lanthanide-free material would be launched perpendicular to the binary midplane. This geometry suggests a viewing angle that is neither edge nor pole on. However, the large velocity (>0.2*c*) we infer for the blue component might make obscuration difficult, and it is unclear if certain viewing angles and ejecta distributions can satisfy all the constraints from the spectral evolution we observe.

The detailed spectral, kinematic, and chemical data obtained for SSS17a provide multiple constraints for understanding binary neutron star mergers. We find that existing models related to neutron star ejecta may explain some aspects of the spectral evolution we present, but no single model matches all of the main properties. The ejecta likely have a complicated, three-dimensional structure, with large internal variations in velocity and composition, and this complexity may be required to account for the full time-series spectral data in greater detail. However, alternative physical mechanisms should not be discounted, especially for the early, hot, thermal emission. The smooth spectrum of the very early optical emission allows us to rule out models, namely disk winds, that would be degenerate with photometry alone.

REFERENCES AND NOTES

1. B. Paczynski, *Astrophys. J.* **308**, L43 (1986).
2. D. Eichler, M. Livio, T. Piran, D. N. Schramm, *Nature* **340**, 126–128 (1989).
3. W. Fong, E. Berger, R. Margutti, B. A. Zauderer, *Astrophys. J.* **815**, 102 (2015).
4. L.-X. Li, B. Paczyński, *Astrophys. J.* **507**, L59–L62 (1998).
5. S. R. Kulkarni, arXiv:astro-ph/0510256 [astro-ph] (10 October 2005).
6. B. D. Metzger *et al.*, *Mon. Not. R. Astron. Soc.* **406**, 2650–2662 (2010).
7. L. F. Roberts, D. Kasen, W. H. Lee, E. Ramirez-Ruiz, *Astrophys. J.* **736**, L21 (2011).
8. B. D. Metzger, *Living Rev. Relativ.* **20**, 3 (2017).
9. E. M. Burbidge, G. R. Burbidge, W. A. Fowler, F. Hoyle, *Rev. Mod. Phys.* **29**, 547–650 (1957).
10. A. G. W. Cameron, *Publ. Astron. Soc. Pac.* **69**, 201 (1957).
11. Y.-Z. Qian, G. J. Wasserburg, *Phys. Rep.* **442**, 237–268 (2007).
12. M. Arnould, S. Goriely, K. Takahashi, *Phys. Rep.* **450**, 97–213 (2007).
13. N. R. Tanvir *et al.*, *Nature* **500**, 547–549 (2013).
14. E. Berger, W. Fong, R. Chornock, *Astrophys. J.* **774**, L23 (2013).
15. M. M. Kasliwal, O. Korobkin, R. M. Lau, R. Wollaeger, C. L. Fryer, *Astrophys. J.* **843**, L34 (2017).
16. D. Kasen, N. R. Badnell, J. Barnes, *Astrophys. J.* **774**, 25 (2013).
17. J. Barnes, D. Kasen, *Astrophys. J.* **775**, 18 (2013).
18. M. Tanaka, K. Hotokezaka, *Astrophys. J.* **775**, 113 (2013).
19. D. Kasen, R. Fernández, B. D. Metzger, *Mon. Not. R. Astron. Soc.* **450**, 1777–1786 (2015).
20. LIGO/Virgo collaboration, *GRB Coordinates Network* 21509 (2017).
21. GBM-LIGO, *GRB Coordinates Network* 21506 (2017).
22. INTEGRAL, *GRB Coordinates Network* 21507 (2017).
23. One-Meter Two-Hemisphere (1M2H) collaboration, *GRB Coordinates Network* 21529 (2017).
24. D. A. Coulter *et al.*, *Science* **358**, 1556–1558 (2017).
25. W. L. Freedman *et al.*, *Astrophys. J.* **553**, 47–72 (2001).
26. M. R. Drout *et al.*, *Science* **358**, 1570–1574 (2017).
27. M. R. Drout *et al., GRB Coordinates Network* 21547 (2017).
28. Materials and methods are available as supplementary materials.
29. Z. Cano, S.-Q. Wang, Z.-G. Dai, X.-F. Wu, *Adv. Astron.* **2017**, 8929054 (2017).
30. E. M. Levesque *et al.*, *Mon. Not. R. Astron. Soc.* **401**, 963–972 (2010).
31. N. R. Tanvir, *et al., GRB Coordinates Network Circular Service* 11123 (2010).
32. A. Cucchiara *et al.*, *Astrophys. J.* **777**, 94 (2013).
33. A. de Ugarte Postigo *et al.*, *Astron. Astrophys.* **563**, A62 (2014).
34. C. D. Kilpatrick *et al.*, *Science* **358**, 1583–1587 (2017).
35. A. Murguia-Berthier *et al.*, *Astrophys. J.* **848**, L34 (2017).
36. M. R. Drout *et al.*, *Astrophys. J.* **794**, 23 (2014).
37. F. Patat *et al.*, *Astrophys. J.* **555**, 900–917 (2001).
38. K. Z. Stanek *et al.*, *Astrophys. J.* **591**, L17–L20 (2003).
39. B. D. Metzger, R. Fernández, *Mon. Not. R. Astron. Soc.* **441**, 3444–3453 (2014).
40. S. Wanajo *et al.*, *Astrophys. J.* **789**, L39 (2014).
41. D. Kasen, B. Metzger, J. Barnes, E. Quataert, E. Ramirez-Ruiz, *Nature* **551**, 80–84 (2017).
42. P. E. Nugent *et al.*, *Nature* **480**, 344–347 (2011).
43. B. J. Shappee *et al.*, *Astrophys. J.* **826**, 144 (2016).
44. R. M. Quimby *et al.*, *Astrophys. J.* **666**, 1093–1107 (2007).
45. R. Pereira *et al.*, *Astron. Astrophys.* **554**, A27 (2013).
46. M. R. Drout *et al.*, *Astrophys. J.* **774**, 58 (2013).

ACKNOWLEDGMENTS

We thank J. Mulchaey (Carnegie Observatories director), L. Infante (Las Campanas Observatory director), and the entire Las Campanas staff for their dedication, professionalism, and excitement, which were critical for obtaining the observations used in this study. B.J.S., M.R.D., K.A., and A.P.J. were supported by NASA through Hubble Fellowships awarded by the Space Telescope Science Institute, which is operated by the Association of Universities for Research in Astronomy, Inc., for NASA, under contract NAS 5-26555. B.J.S. and E.B. were supported by Carnegie-Princeton Fellowships. M.R.D. was supported by a Carnegie-Dunlap Fellowship and acknowledges support from the Dunlap Institute at the University of Toronto. T.W.-S.H. was supported by a Carnegie Fellowship. Support for J.L.P. was in part provided by the Fundo Nacional de Desarrollo Científico y Tecnológico (FONDECYT) through grant 1151445 and by the Ministry of Economy, Development, and Tourism's Millennium Science Initiative through grant IC120009, awarded to the Millennium Institute of Astrophysics. D.K. is supported in part by a U.S. Department of Energy (DOE) Early Career award DE-SC0008067, a DOE Office of Nuclear Physics award DE-SC0017616, and a DOE SciDAC award DE-SC0018297, and by the Director, Office of Energy Research, Office of High Energy and Nuclear Physics, Divisions of Nuclear Physics, of the DOE under contract no. DE-AC02-05CH11231. V.M.P. acknowledges partial support for this work from grant PHY 14- 30152 from the Physics Frontier Center, JINA–Center for the Evolution of the Elements (JINA-CEE), awarded by the NSF. The University of California–Santa Cruz (UCSC) group was supported in part by NSF grant AST-1518052, the Gordon and Betty Moore Foundation, the Heising-Simons Foundation, generous donations from many individuals through a UCSC Giving Day grant, and from fellowships from the Alfred P. Sloan Foundation (R.J.F.), the David and Lucile Packard Foundation (R.J.F. and E.R.-R.), and the Niels Bohr Professorship from the Danish National Research Foundation (E.R.-R.). T.B. acknowledges support from the Consejo Nacional de Ciencia y Tecnologia (CONACYT) Research Fellowships program. G.M. acknowledges support from Comisión Nacional de Investigación Científica y Tecnológica (CONICYT), Programa de Astronomía–Programa de Cooperación Internacional, FONDO ALMA 2014, project no. 31140024. A.M.-B. acknowledges support from a University of California Institute for Mexico and the United States (UC MEXUS)–CONACYT Doctoral Fellowship. C.A. was supported by Caltech through a Summer Undergraduate Research Fellowship (SURF) with funding from the Associates SURF Endowment. J.X.P. is also affiliated with the Kavli Institute for the Physics and Mathematics of the Universe. This paper includes data gathered with the 6.5-m Magellan Telescopes located at Las Campanas Observatory, Chile. Part of this work is based on a comparison to observations of GRB130603B that were obtained from the European Organisation for Astronomical Research in the Southern Hemisphere (ESO) Science Archive Facility under request number vmplacco308387. We thank A. Cucchiara for sending us the spectrum of GRB130603B. We thank J. van Saders for useful suggestions. We thank the University of Copenhagen, Dark Cosmology Centre, and the Niels Bohr International Academy for hosting D.A.C., R.J.F., A.M.-B., E.R.-R., and M.R.S. during a portion of this work. R.J.F., A.M.-B., and E.R.-R. were participating in the Kavli Summer Program in Astrophysics, "Astrophysics with gravitational wave detections." This program was supported by the Kavli Foundation, Danish National Research Foundation, the Niels Bohr International Academy, and the Dark Cosmology Centre. This research has made use of the NASA/IPAC Extragalactic Database (NED), which is operated by the Jet Propulsion Laboratory, California Institute of Technology, under contract with NASA. The data presented in this work and the code used to perform the analysis are available at https://data.obs.carnegiescience.edu/SSS17a/. Calibrated rest-wavelength spectra are also made available at the Weizmann Interactive Supernova Data Repository (WISeREP) (doi:10.1086/666656; https://wiserep.weizmann.ac.il/).

SUPPLEMENTARY MATERIALS

www.sciencemag.org/content/358/6370/1574/suppl/DC1
Materials and Methods
Fig. S1
Tables S1 and S2
References (*47–63*)

22 September 2017; accepted 11 October 2017
Published online 16 October 2017
10.1126/science.aaq0186

Science

Early spectra of the gravitational wave source GW170817: Evolution of a neutron star merger

B. J. Shappee, J. D. Simon, M. R. Drout, A. L. Piro, N. Morrell, J. L. Prieto, D. Kasen, T. W.-S. Holoien, J. A. Kollmeier, D. D. Kelson, D. A. Coulter, R. J. Foley, C. D. Kilpatrick, M. R. Siebert, B. F. Madore, A. Murguia-Berthier, Y.-C. Pan, J. X. Prochaska, E. Ramirez-Ruiz, A. Rest, C. Adams, K. Alatalo, E. Bañados, J. Baughman, R. A. Bernstein, T. Bitsakis, K. Boutsia, J. R. Bravo, F. Di Mille, C. R. Higgs, A. P. Ji, G. Maravelias, J. L. Marshall, V. M. Placco, G. Prieto and Z. Wan

Science **358** (6370), 1574-1578.
DOI: 10.1126/science.aaq0186originally published online October 16, 2017

Photons from a gravitational wave event

Two neutron stars merging together generate a gravitational wave signal and have also been predicted to emit electromagnetic radiation. When the gravitational wave event GW170817 was detected, astronomers rushed to search for the source using conventional telescopes (see the Introduction by Smith). Coulter *et al.* describe how the One-Meter Two-Hemispheres (1M2H) collaboration was the first to locate the electromagnetic source. Drout *et al.* present the 1M2H measurements of its optical and infrared brightness, and Shappee *et al.* report their spectroscopy of the event, which is unlike previously detected astronomical transient sources. Kilpatrick *et al.* show how these observations can be explained by an explosion known as a kilonova, which produces large quantities of heavy elements in nuclear reactions.

Science, this issue p. 1556, p. 1570, p. 1574, p. 1583; see also p. 1554

Science (print ISSN 0036-8075; online ISSN 1095-9203) is published by the American Association for the Advancement of Science, 1200 New York Avenue NW, Washington, DC 20005.

Science (print ISSN 0036-8075; online ISSN 1095-9203) is published by the American Association for the Advancement of Science, 1200 New York Avenue NW, Washington, DC 20005.